

Applications of Statistical Imaging of the Sea using a Robotic Telescope

Anthony Cook¹, Martin Vickers¹ and Grant Stevens-Bulmer¹

¹*Institute of Mathematics and Physics, Aberystwyth University, Aberystwyth, SY23 3BZ
Email: atc@aber.ac.uk*

Summary

We investigate the feasibility of shore-based, time lapse video, for the detection and imaging of sea surface states and objects. Temporal monitoring a fixed area of the sea yields images that represent a statistical population of sea surfaces, or object aspects. The sea brightness histogram will range from bright surf or sun-glint, down to dark wave troughs. By obtaining a temporal sequence of images, stacking these into a data cube and then applying statistical imaging we can select pixels with minimum or maximum interference from waves. This enables us to detect any object that a wave breaks against, or dark low lying objects that occasionally protrude through the sea surface. We also see any floating object with apparent motions generated from a variety of sources such as wind. Once an object has been detected, a second statistical imaging technique, known as “Lucky Imaging” can be used to remove the blurring effects in the Earth’s atmosphere. In future we plan to use our robotic telescope to scan the sea surface and return the range, altitude and azimuth angles of any sea surface object within the image. Possible applications of the statistical imaging might include mapping sea colour and roughness, the detection of submerged wrecks, automated tracking of boats and individuals getting into difficulty, monitoring of wild-life and high resolution imaging of vessels for defence.

1 Introduction

Whilst robotic telescopes have been used extensively in a number of night time astronomical applications, such optical flash detection from Gamma Ray Bursters (Wren. *et al*, 2002), their application to terrestrial daylight close range remote sensing is rarely utilized. The distances over which telescopic imaging can function range from ~100m (focussing limits), out to tens of kilometres, constrained by the Earth’s curvature (Lerczak and Hobbs, 1998). From our observatory (h=139m GPS reading), the sea-surface horizon is 45km away (terrestrial refraction). In comparison with nadir remote sensing from orbit, ground based close range remote sensing, suffers disadvantageous image degradation due to larger optical depths, atmospheric turbulence, refraction and scene foreshortening. However we demonstrate means to overcome some of these issues and also illustrate the advantages of high resolution temporal imagery. We have not constructed an end-to-end automated system at the time of writing, but describe many of the steps involved.

2 Equipment

We use a 267mm aperture Meade telescope (Cook, 2008), with a focal reducer that provides an image scale of 1.96”/pixel. Time lapse 640x480 images are captured to an AVI file from a Watec 902H 0.0003 Lux, CCTV camera with filter wheel. A near IR filter offers optimum image contrast with reduced Rayleigh scattering from the sky (Bohren and Huffman, 1983) making most objects and surf, on the sea, appear contrasty against the darker sea background.

3 Methodology

Figure 1 shows the key components of our system in development, and has been included to illustrate functionality. The basic steps involved are:

- Image navigation, to determine the coordinates of the area of sea being imaged.
- Images acquisition
- Temporal statistical analysis performed to extract imagery of the sea surface state.
- If an object is present in the scene, such as a boat, then its orientation and position against the sea surface should be determined, and Lucky Imaging (Law *et al.*, 2006) applied to extract sharper detail.

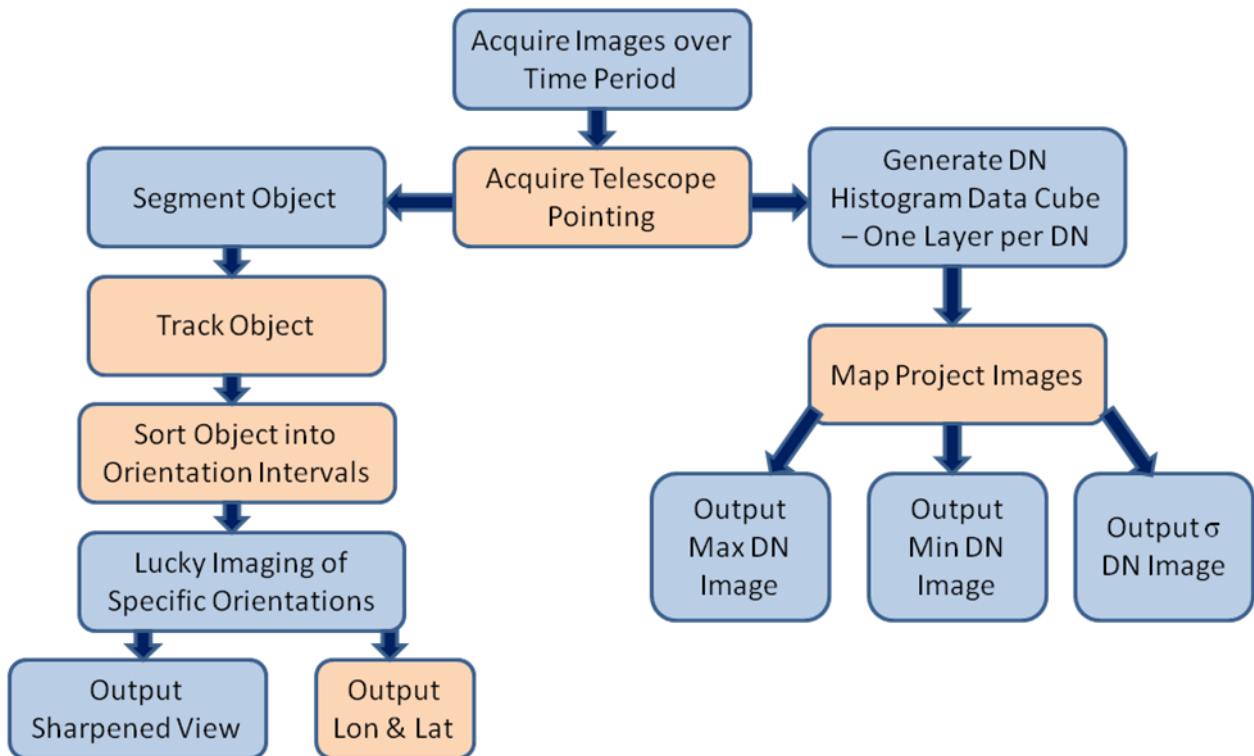


Figure 1. Flow chart of our proposed system. Blue boxes illustrate demonstrated steps. Areas still under investigation are in light orange.

3.1 Object Azimuth and Range

The telescope that we use has an Alt-Az axes but the control software both locates and displays objects according to Right Ascension (RA) and Declination (Dec). Calibration of the telescope pointing capabilities can be done either at night using stars to $\sim 1'$ accuracy, or to $\sim 1^\circ$ during daytime based purely upon GPS, magnetic north and automatic levelling. We will discuss ways to improve daylight pointing accuracy in section 5.

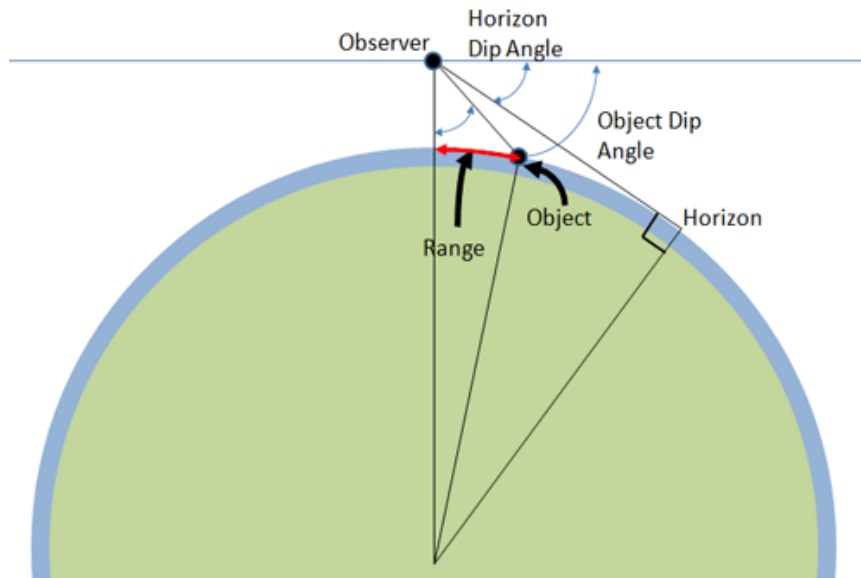


Figure 2. Range determination geometry of objects at sea (Gailey and Ortega-Ortiz, 2000).

Figure 2 illustrates that if we know the sea surface model to a first order (assumed to be a shell of thickness equivalent to the tidal height), then if we know the dip angle from the horizontal, the range may be calculated – see Gailey and Ortega-Ortiz (2000). Terrestrial refraction effects will apply, but are only appreciable at distances approaching the horizon where the amount of refraction is affected by the tropospheric lapse rate.

3.2 Temporal Imaging

For the right hand side of Figure 1 flow chart, for each sample and line location in all the images, we obtain a 256 grey level histogram. This is stored in an $NS \times NL \times 256$ 3D array, where NS and NL correspond to the number of lines and samples in each image. The 256 layers in this data cube hold the frequency of specific DN values at that given image pixel. This arrangement permits us to calculate the minimum, maximum and brightness standard deviation of each pixel in the original images (Figure 4).

3.3 Object Characteristic

In order to proceed to section 3.4, it is necessary to extract objects, such as boats, from a scene and sort them by pitch, yaw, roll (Figure 3) and also determine the image scale. Suitable angular bin intervals are allocated, e.g. 5° , so that images placed into each bin appear similar. It is advisable to use parts of the object that are well out of the water, for example the mast or a cabin structure, in order to avoid hidden detail from waves. Images in the most populated bins can then go into the Lucky Imaging algorithm. Image scales are discussed in sections 4.3-4.4.

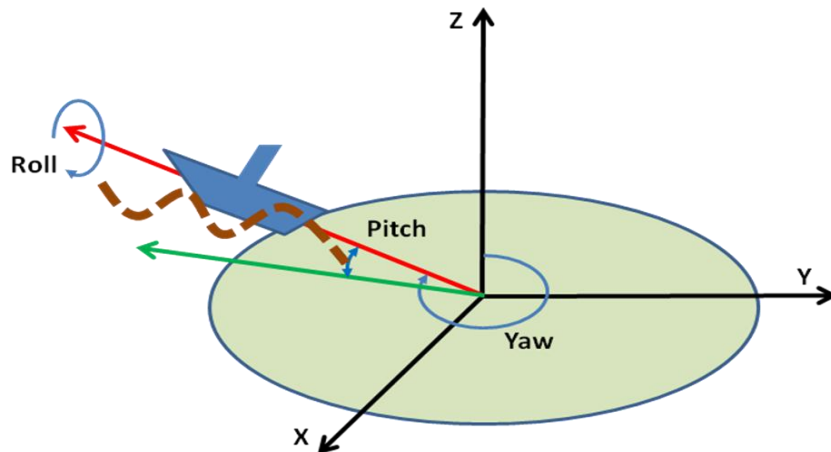


Figure 3. The effects of pitch, roll and yaw on the apparent orientation and aspect ratio of a ship. A change in yaw, away from the Y axis, will shorten the apparent angular length of the ship, but leave apparent height unchanged.

3.4 High Resolution Lucky Imaging

The basis behind Lucky Imaging (Law, Mackay and Baldwin, 2006) is that light from a perfect distant scene has passed through our turbulent atmosphere and results in an image distorted and blurred by different amounts related to the power spectrum and isoplanar patch sizes of the atmospheric convection cells. Astronomers have found that if you take enough short exposure images, then a small proportion are relatively sharp. Therefore if images can be selected according to their sharpness criteria e.g. the top 10%, and then registered together, stacked and combined to improve signal to noise ratio, then it is possible to recover a sharp and representative example image of the original scene. We utilize RegiStax (<http://www.astronomie.be/registax/index.html>) freeware in our experiments.

4 Results

The following subsections illustrate part of our eventual goals and also potential applications of the technique.

4.1 Wave Breaking and Surf

Figure 4 was obtained with just a camcorder, but highlights (top and bottom right) how to pick out “breaking waves” via maximum DN or standard deviation DN. The former is prone however to transient bright artefacts such as sea gulls, or sun glint. It may be possible though to filter these effects out by not using the brightest DN value at a given pixel, but say 5% closest to the brightest value.



Figure 4. Temporal processing on sea images. (Top Left) One of the original images. (Top Right) Maximum DN at a given pixel – the wiggly lines are sea gull take offs and landings. (Bottom left) Minimum DN. (Bottom Right) Standard deviation DN. From Vickers (2006).

4.2 Low Lying Objects

Low lying objects can be detected, even though they may be visible less than 1% of the time. The reflectivity of such objects is generally less than the sea surface, so therefore if one waits long enough and looks for the darkest DN value at a given pixel, then we can map the sea in a quiet state, often at its lowest level. Figure 4 (lower left) illustrates that the triangular structure has a larger visible area than it has in the upper images. There are also several smaller undersea posts visible. The technique is not perfect though as it has also detected sea gull shadows.

4.3 Wave Heights

To illustrate wave height measuring capability, a buoy, was imaged at regular intervals in NIR. The buoy top image pixel position was monitored over time with respect to an origin, defined as an angled roof section of a house (Figure 5). The dip angle to the buoy, from the horizontal was 3.79° and the distance to the buoy was $\sim 2.1\text{km}$ giving an image scale of $\sim 2\text{cm/pixel}$. Figure 6 shows the measured position of the buoy top as a function of time. The peak to trough wave extreme was $\sim 25\text{cm}$, and the main wave periodicity was ~ 4 seconds with a hint of a longer ~ 15 sec period. However it is likely that there is also some noise present from image distortion due to atmospheric turbulence.

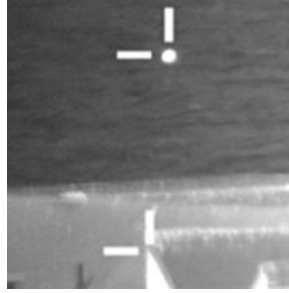


Figure 5. Section of image used to measure the wave height of the buoy. The lower and upper markers define the origin and the buoy.

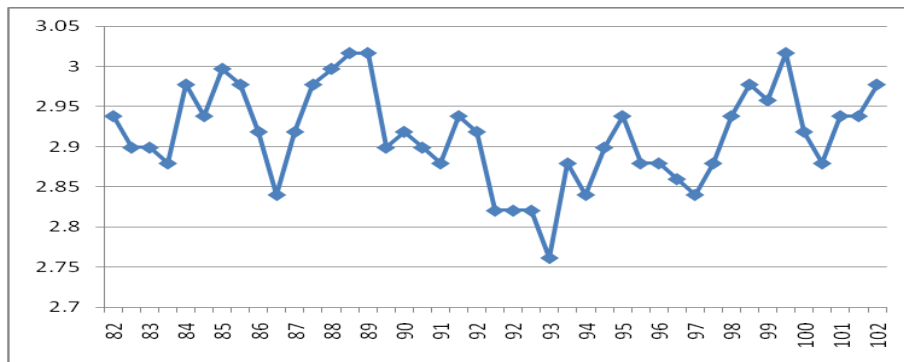


Figure 6. The vertical axis is the cm wave height of the buoy. The horizontal axis is time in seconds.

4.4 Lucky Imaging of Boats

To demonstrate the ability of Lucky Imaging to extract non-atmospheric seeing blurred images of objects, video was captured of a fishing boat. Due to changing aspect and orientation of the boat in the sea, pre-processing was used to isolate the most common base to height ratio of the vessel. A resulting 59 images were deemed suitable and fed into RegiStax – an example source image can be seen in Figure 7 (left). The top 10% quality remaining image frames were selected and used to produce an appreciably deblurred image in Figure 7 (right).

Although we did not identify the boat concerned, it is possible to estimate the distance D thus:

- The image scale of the camera was 0.000544° /pixel
- The cabin height measured 60 pixels in the image
- Assume the cabin had a height of 1.8m
- The image scale at distance D was therefore $\sim 3\text{cm}/\text{pixel}$
- The boat distance $D = 0.03 / \text{Tan}(0.000544^\circ) = 3160\text{m}$ or 3.2km



Figure 7. (Left) One of the original images. (Right) Image produced, after Lucky Imaging. From Stevens-Bulmer (2009).

5 Discussion

We have summarized a statistical based imaging system that we have been working on, through example stages involved. As yet an end to end system has not been completed, but from the limited set of results, it is apparent that this could be a practical measuring and monitoring tool for a wide variety of applications. Stereo based methods (Schimmels *et al.*, 2005) are the most accurate way to measure wave heights, however our approach can cover a larger area and at greater distances. We intend to investigate the robustness of the system, in particular searching for and tracking individuals or boats getting into difficulty at sea, automated detection and monitoring of surfacing Cetaceans, attempting to identify birds from the loci of their take offs and landings (see Figure 4 top right), and whether the filters can be used to map out river-sea water boundaries or pollution.

Several issues remain to be solved, for example how to improve daytime pointing accuracy? This might be achievable by using geographical landmarks, or by leaving a night time calibrated telescope running into daytime. Another issue is how to filter out atmospheric turbulence and telescope wind shake from wave frequencies, especially when we move far off shore away from fixed reference points. A frequency spectrum approach is being considered?

One final thought, we have so far not attempted to work at the diffraction limited resolution of the telescope. In theory at 550nm this should be 0.00014° or $0.5''$ using $1.22\lambda/D$ (where D is the diameter of the telescope, and λ is the wavelength of light), however over sampling would be needed to cater for the Modulation Transfer Function.

References

- BOHREN, C.F. and HUFFMAN, D., 1983. Absorption and Scattering of Light by Small Particles, John Wiley, New York.
- COOK, A.C., 2008 Aberystwyth University Robotic Telescope Web page, http://users.aber.ac.uk/atc/Robotic_telescopes.htm
- GAILEY, G., and ORTEGA-ORTIZ, J., 2000. PYTHAGORAS Theodolite Cetacean Tracking, Marine Mammal Research Program, Texas A&M University at Galveston.
- LAW, N. M., MACKAY, C. D., & BALDWIN, J. E., 2006. Lucky imaging: high angular

- resolution imaging in the visible from the ground. *Astronomy and Astrophysics*, **446**: 739-745.
- LERCZAK, J. A., and HOBBS, R.C.. 1998. Calculating sighting distances from angular readings during shipboard, aerial, and shore-based marine mammal surveys, *Marine Mammal Science*, **14**(3):590-599.
- SCHIMMELS, V.S., SANTEL, F., ZIELKE, W. and HEIPKE, C., 2005. WAVESCAN – Automatisierte Erfassung und odellierung von Brandungszonen auf Basis digitaler Bildsequenzen. In: KFKI aktuell- German Coastal Engineering Research Council – GCERC newsletter, 3th year Edition, Hamburg, 02/2004-2005, 2-4.
- STEVENS-BULMER, G., 2009. Imaging objects at sea using a robotic telescope, MPhys Institute of Mathematical and Physical Sciences, Aberystwyth University.
- VICKERS, M.J., 2006. Baywatch “An automated life guard system”, BSc Computer Science Dissertation, University of Nottingham.
- WREN, J. *et al.*, 2002. A Distributed Control System for Rapid Astronomical Transient Detection, *Proceedings of SPIE*, 4845-21.